PERGAMON

Scripta mater. 42 (2000) 645–651

Scripta MATERIALIA

www.elsevier.com/locate/scriptamat

ATOMIC-SCALE STUDY OF SECOND-PHASE FORMATION INVOLVING LARGE COHERENCY STRAINS IN Fe–20 at.% Mo

Dieter Isheim[1], Olof C. Hellman[1], David N. Seidman[1], Frédéric Danoix[2] and Didier Blavette[2]

[1] Department of Materials Science and Engineering, Northwestern University, Evanston, IL 60208 USA [2] Groupe de Métallurgie Physique, UMR CNRS 6634, Faculté des Sciences de Rouen, F-76821 Mont Saint Aignan Cedex, France

(Received August 9, 1999)
(Accepted October 19, 1999)

Keywords: Microstructure; Homogeneous phase transformation; Transmission electron microscopy; Field ion microscopy; Atom probe

Introduction

The constraint of a coherent interface between a homogeneously precipitating phase and its matrix is known to have a strong influence on the decomposition trajectory and microstructure. The selection of the phase, shape, and composition of the precipitates, as well as their spatial distribution, depend on the volume strain and interfacial free energy associated with the coherent interface. These effects have been studied predominantly by transmission electron microscopy (TEM) (1,2) and by computer simulations based on various models and numerical approaches (3,4,5). The three-dimensional nature of strain-influenced microstructures, however, makes an experimental characterization extremely difficult. The present work investigates the strain dominated precipitate microstructure in an Fe–20 at.% Mo alloy, aged at 500°C for 20 h, resolved in three dimensions (3D), on an atomic scale, by 3D-atom-probe microscopy (3D-APM).

The Fe-Mo system has a difference in atomic volume of about 27% between the elements; Thus, coherency strains are expected to have significant effects. References (6–8) report on the development of a tweed-like modulated strain-contrast in TEM images after annealing an Fe–20 at.% Mo alloy, indicating a periodic decomposition microstructure. Previous investigations by atom-probe field-ion microscopy (APFIM) in combination with high resolution electron microscopy (HREM) (7,8) revealed that homogeneous decomposition of this alloy proceeds during the initial stages via the formation of metastable and coherent Mo-rich bcc precipitates. The four intermetallic phases of the Fe-Mo equilibrium phase diagram (9) are bypassed during the initial stages of the decomposition due to the kinetic constraint of a coherent interface (8). The Fe-Mo system thus constitutes an example of a kinetically determined metastable phase with a composition very different from the phase predicted by the equilibrium phase diagram. The coherency during the initial stages and the large lattice parameter misfit of 7.15% between the Mo-rich precipitate and Fe-rich matrix result in large strain energy effects on the decomposition microstructure. The present work investigates the 3D alignment of the decomposition microstructure in Fe–20 at.% Mo by 3D-APM. This experimental technique reconstructs in three

PII: S1359-6462(99)00412-1

dimensions a specimen volume of typically $15 \times 15 \times 50$ nm^3, based on the spatial coordinates and the chemical identity of each detected atom.

Experimental

An Fe–20 at.% Mo alloy was prepared by arc-melting from pure Fe and pure Mo. Small pieces of the ingot were melted using an electromagnetic levitation coil and then rapidly solidified by the anvil-and-piston splat quenching technique to ensure chemical homogeneity. The composition of the resulting sheets, $\approx$40 μm thick, was determined at several locations by electron microprobe analysis to be 20 $\pm$ 0.2 at.% Mo. Strips $\approx 5 \times 0.1 \times 0.04$ mm^3 in size were cut from the sheets to prepare FIM tips. These strips were then isothermally aged at 500°C for 20 h in Ar. Subsequently, the strips were mechanically ground to a $\approx 0.04 \times 0.04$ mm^2 cross-section and then electropolished in a solution of 5 vol.% perchloric acid in butoxyethanol at 15–12 V DC at room temperature. TEM foils were prepared using a Struers double-jet electropolisher and a solution of 10 vol.% perchloric acid in acetic acid at 25 V DC and 11°C.

3D-APM was performed using the tomographic atom probe (TAP) at the University of Rouen (10). The spatial resolution is typically one atomic layer ($\approx$0.2 nm) in the direction in which the analysis is carried out, the depth direction, and 0.5 nm laterally. The depth scale was calibrated with a set of (110)-planes resolved by the 3D reconstruction process. The detection efficiency of the TAP is about 50%, i.e. approximately 50% of the atoms of the original specimen volume appear in the reconstruction. 3D-APM was performed with the tip at a temperature of 80 K, employing a pulse-voltage-to-total-voltage ratio of 0.19 in a residual gas pressure of $5 \cdot 10^{-8}$ Pa.

Results and Discussion

TEM of an Fe–20 at.% Mo alloy aged at 500°C for 20 h, using dynamical two-beam conditions, detects a somewhat irregular, tweed-like modulated strain-contrast pattern, Fig. 1, with a preferred orientation along the matrix's <100>-type directions and a characteristic grid pitch of about 6 nm. The enlarged (110)-reflection in a diffraction pattern, Fig. 2, exhibits diffuse streaks in the <100>-type directions with a tendency toward satellite-like intensity shoulders. The maxima of these intensity shoulders appear at approximately 1/40 (200) in reciprocal space, which corresponds to a characteristic length scale in real space of about 6 nm, in agreement with the grid pitch of the tweed-pattern in real space images, Fig. 1. These TEM results indicate that a coherent second phase with considerable coherency strains is formed, in agreement with previous studies of the decomposition of Fe–20 at.% Mo (6,7,8).

Different representation methods are utilized to visualize the 3D-APM data. Fig. 3 displays the 40 at.% Mo isoconcentration surface of a reconstructed volume, originally $19 \times 19 \times 58$ nm^3 in size, obtained from an Fe–20 at.% Mo alloy aged at 500°C for 20 h. Isoconcentration surfaces interpolate through a field of concentration values at a specified concentration level. Concentration values are obtained by dividing the number of atoms of one atomic species by the number of all atoms contained in a sampling volume of fixed size, surrounding a respective coordinate. As this is essentially spatial averaging and because of the interpolation scheme used, closely spaced precipitates might not be separated by isoconcentration surfaces. Thus, at the 40 at.% Mo level, the Mo-enriched precipitates appear as an interconnected structure, thereby accentuating the three-dimensional nature of the microstructure. The Mo-rich precipitates are aligned into chain-like structures along the cubic <100>-type directions, which in Figure 3 are approximately parallel to the largest dimension (depth direction) of the reconstructed volume and to the diagonals of its square cross-section.

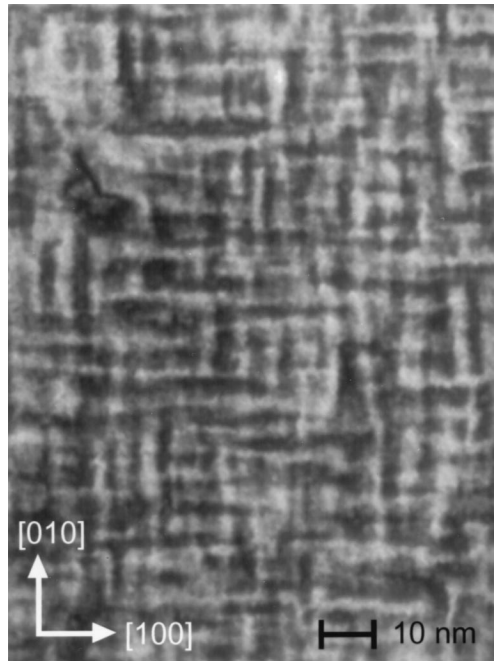

Figure 1. Tweed-like strain contrast in a bright-field TEM image of Fe–20 at.% Mo after aging a specimen at 500°C for 20 h.

Details of the precipitate chain in the upper portion of Fig. 3 are revealed atom-by-atom in Fig. 4, which displays nine successive slices, each 1 nm thick, cut horizontally from the reconstructed volume as indicated in the upper portion of Fig. 3. Stepping through the series of slices reveals that the chain consists of individual Mo-rich precipitates, separated by Fe-rich layers. The centroids of the Mo-rich

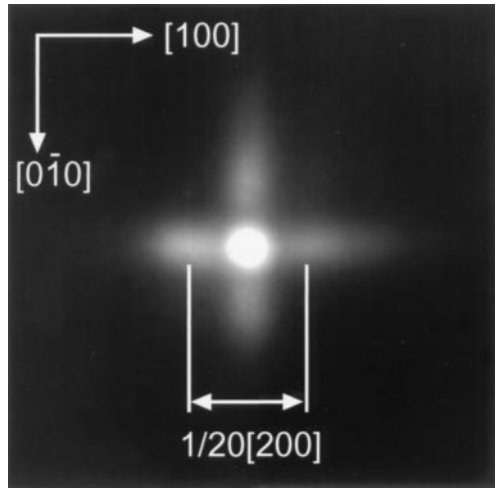

Figure 2. Enlarged (110)-reflection of an electron diffraction pattern of an Fe–20 at.% Mo specimen aged at 500°C for 20 h. Diffraction pattern recorded with the incident beam close to the [001]-zone axis.

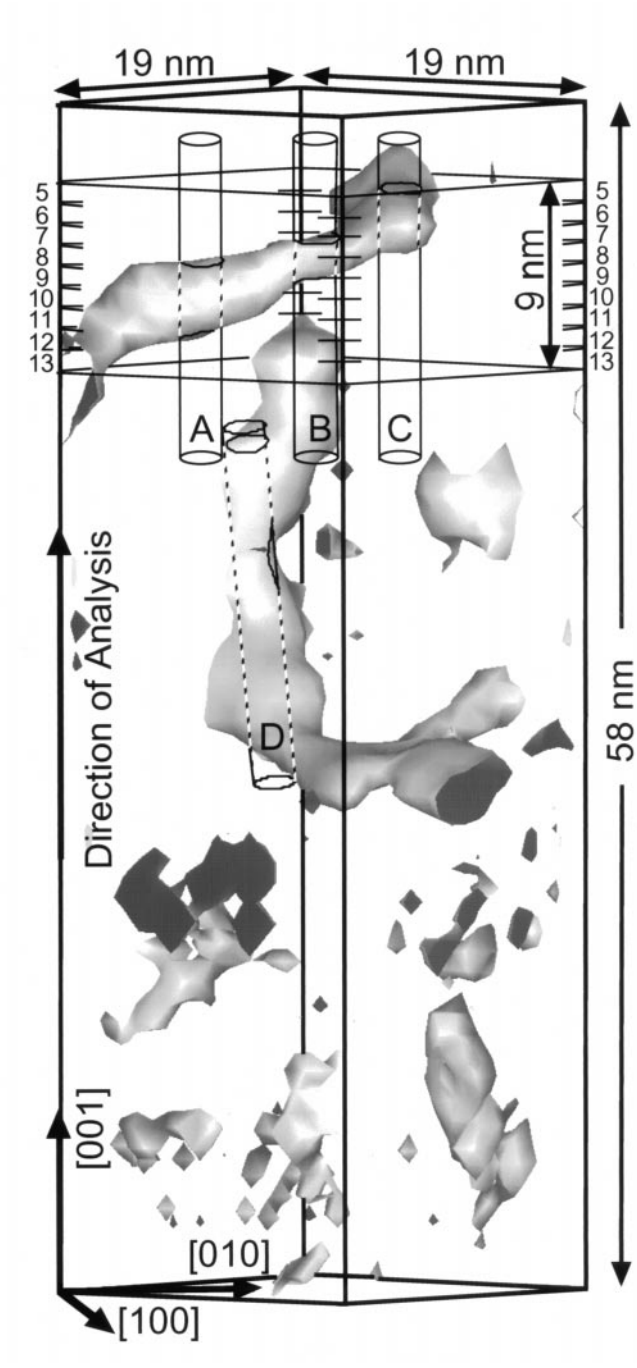

Figure 3. 40 at.% Mo isoconcentration surface from a 3D-APM analysis of an Fe–20 at.% Mo specimen aged at 500°C for 20 h. The size of the reconstructed volume is $19 \times 19 \times 58$ nm^3. The <100> directions are approximately oriented along the long axis of the volume and the diagonals of the square cross-section.

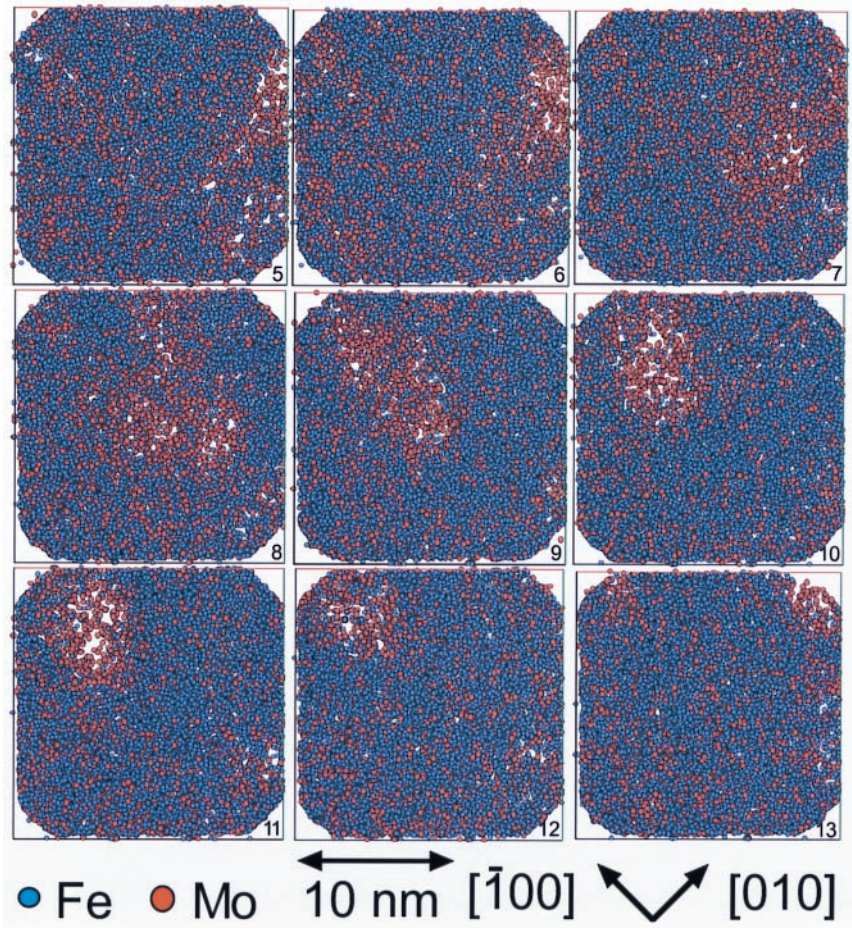

Figure 4. Reconstructed atomic positions for Mo-atoms (red) and for Fe (blue) from a 3D-APM analysis of an Fe–20 at.% Mo specimen aged at 500°C for 20 h. Sequence of nine successive slices of 1 nm thickness cut horizontally, perpendicular to the [001]-depth direction, from the upper part of the reconstructed volume represented in Fig. 3 as indicated by labels 5 through 13. Stacked on top of each other, the total volume of the slices is $19 \times 19 \times 9$ nm^3. Stepping through the series reveals a chain of Mo-rich particles, spearated by Fe-rich regions.

regions are about 5–7 nm apart, in agreement with the characteristic length scale of 6 nm determined from electron diffraction patterns.

The atomic density appears reduced within the Mo-rich areas. This results partly from the larger atomic volume of Mo and to a larger extent from an additional lateral magnification of the Mo-rich precipitates caused by the higher evaporation-field strength of the Mo-rich precipitates. This results in a protrusion of the Mo-rich precipitates from the approximately hemispherically shaped surface of an FIM tip's apex. As the local curvature of a tip's surface is inversely proportional to the magnification, the Mo-rich regions are laterally more highly magnified, thereby causing a lateral distortion. In order to obtain quantitatively scaled concentration profiles, the precipitates are therefore probed approximately along the [001]-depth direction of the analyzed volume, which is parallel to the tip axis and thus not affected by the additional lateral magnification.

Figures 5(a)–(d) display concentration profiles recorded across precipitates as indicated by the probing cylinders marked in Fig. 3 with the letters A – D. The precipitates, 2–4 nm in diameter, have

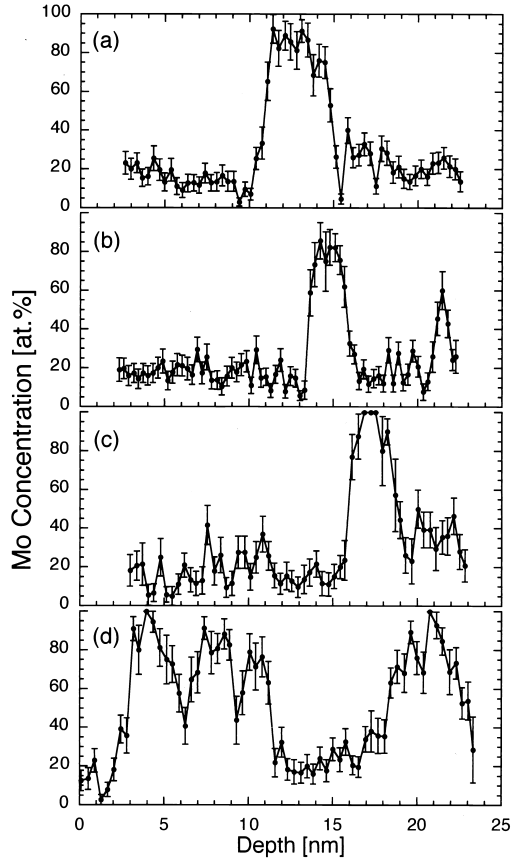

Figure 5. (a)-(d). Concentration profiles across Mo-rich precipitates in an Fe–20 at.% Mo alloy aged at 500°C for 20 h, recorded along the probe cylinders A-D indicated in Fig. 3. Concentration profile (d) reveals a chain of very closely spaced precipitates, separated by Fe-rich interlayers. The error bars indicate the standard deviation $\sqrt{c(1-c)/N}$, with c the measured concentration and N the number of atoms entering the concentration calculation.

an Mo concentration of 80–100 at.%. Figure 5(d) exhibits a concentration profile along a chain of four precipitates, recorded close to the [001]-direction of analysis with probing cylinder D in Fig. 3. Three of the precipitates are distributed within a range of 6–7 nm, followed by a precipitate at a distance of about 10 nm. The three closely spaced precipitates on the left-hand side of Fig. 5(d) are separated by a thin Fe-rich layer with a thickness of only one or two atomic layers, corresponding to about 0.4 nm. The observed decreases in Mo concentration between the precipitates, to about 40 at.% Mo, are statistically significant and, due to the involved spatial averaging, provide a lower limit of the Fe concentration of the interlayer.

Conclusions

The three-dimensional arrangement of nm-scale precipitates in an Fe–20 at.% Mo alloy, aged at 500°C for 20 h, has been resolved in three dimensions for the first time by 3D-APM. The precipitates have an Mo concentration of about 90 at.% Mo, are 2–4 nm in size, and are arranged in chain-like structures along the <100>-type directions of the bcc Fe-rich matrix. This alignment is caused by coherency

strain, due to the 7.15% misfit between precipitate and matrix, coupled with the elastic anisotropy of the Fe-rich matrix and explains the tweed-like modulated contrast pattern observed by TEM. These results confirm the conclusions of prior APFIM experiments that a metastable, Mo-rich phase forms upon annealing at 500°C.

Acknowledgments

DI thanks the members of the Groupe de Métallurgie Physique, Rouen, France, for their warm hospitality and assistance during his stay. Mr. J. Vandenbroucke is thanked for his contribution to the development of data evaluation software. The provision of the piston-and-anvil quencher of the Lehrstuhl für Physik I, Universität Augsburg, Germany, by Professor K. Samwer is gratefully acknowledged. This research was supported by the National Science Foundation, Division of Materials Research (Dr. B. MacDonald, grant officer), the Deutsche Forschungsgemeinschaft, and the Alexander von Humboldt Foundation through the Max Planck research prize of DNS.

References

1. A. J. Ardell, R. B. Nicholson, and J. D. Eshelby, Acta Metall. 14, 1295 (1966).
2. T. Miyazaki, H. Imamura, and T. Kozakai, Mater. Sci. Eng. 54, 9 (1982).
3. C. H. Su and P. W. Voorhees, Acta Mater. 44, 2001 (1996).
4. Y. Wang, L. Q. Chen, and A. G. Khachaturyan, Acta Metall. Mater. 41, 279 (1993).
5. T. Koyama and T. Miyazaki, Mater. Trans. JIM. 39, 169 (1998).
6. T. Miyazaki, S. Takagishi, H. More, and T. Kozakai, Acta Metall. 28, 1143 (1980).
7. D. Isheim, Doctoral Thesis, Georg August Universität Göttingen, Germany (1995).
8. D. Isheim, submitted for publication.
9. A. F. Guillermet, Bull. Alloy Phase Diagr. 3, 359 (1982).
10. D. Blavette, B. Deconihout, A. Bostel, J. M. Sarrau, M. Bouet, and A. Menand, Rev. Sci. Instr. 64, 2911 (1993).